Hydrodynamic friction and the capacitance of arbitrarily shaped objects

Jack F. Douglas,[1] Huan-Xiang Zhou,[2] and Joseph B. Hubbard[3]
[1]*Polymers Division, National Institute of Standards and Technology, Gaithersburg, Maryland 20899*
[2]*Laboratory of Chemical Physics, National Institute of Diabetes and Digestive and Kidney Diseases, National Institute of Health, Bethesda, Maryland 20892*
[3]*Biotechnology Division, National Institute of Standards and Technology, Gaithersburg, Maryland 20899*
(Received 19 November 1993)

The translational friction coefficient and the capacitance of a variety of objects are calculated with a probabilistic method involving hitting the "probed" objects with random walks launched from an enclosing spherical surface. This method is applied to exactly solvable examples to test the program accuracy and to physically important and analytically intractable examples (cube, chain of spheres at the vertices of self-avoiding and random walks, etc.). Large fluctuations in the friction of polymer chains with a random coil structure are found to give large deviations from the mean-field Kirkwood-Riseman theory and "hydrodynamic fluctuation" effects are found to diminish with the chain swelling accompanying excluded volume interaction. Capacity applications are reviewed and our probabilistic estimates of polymer friction are compared with previous calculations using alternative methods. Transients to the capacity and related properties are expressed in terms of fluctuations in the "Wiener sausage" volume (volume swept out by a Brownian particle where a repeated visit to a spatial region does not contribute to the volume increase in time).

PACS number(s): 02.70.Lq, 83.10.Nn, 82.20.Fd

I. INTRODUCTION

There are many physical processes in which the solution of Laplace's equations on the exterior of a body of general shape is central to the theoretical description. The case of a constant boundary condition (the exterior Dirichlet problem) represents a particularly important class of such processes [1]. Although this kind of problem can be readily posed, an analytic solution can be notoriously difficult even for boundaries having simple shapes [1,2]. For example, considerable effort has been made to solve the exterior Dirichlet problem for a cube, leading Pólya [3] to the pessimistic conclusion that there is little hope of obtaining an exact solution. Following the advice of Rayleigh [2], "Yet even when analysis fails to give a solution in the mathematical sense, we need not be altogether in the dark as to the magnitudes of the quantities with which we are dealing," Pólya and Szegö [1,3] embarked on an ambitious program to bound functionals of object shape related to the exterior Laplace equation (capacity, virtual mass, polarization), corresponding to different boundary conditions. Elaborate analysis sets the bounds on the capacity (a central parameter in the exterior Dirichlet problem) of a unit cube to the range [1,3,4] (0.632,0.710 55). The limited progress in improving this bound reflects the intrinsic difficulty of this type of problem.

Solution of the exterior Dirichlet problem is generally limited to shapes related to special coordinate systems in which Laplace's equation is separable [1,5,6]. However, naturally occurring boundaries often do not conform to these simple forms. In the present paper we cast the problem of calculating the capacity in terms of a probabilistic formulation, involving averaging over random walk paths, which allows treatment of boundaries having *arbitrary* shape. Actually this is a classical approach to this type of problem in the mathematical literature [7], but the results obtained have usually been formal in nature. Modern computer resources allow for a direct implementation of this approach to obtain qualitative estimates of capacity.

The number of physical processes related to the exterior Dirichlet problem for Laplace's equation is extensive [1]. Many of these processes are related to the steady-state diffusion of mass, energy, or some other quantity toward or away from a body. The capacity in this context determines the rate of the steady-state flux. In other cases, the physical origin of the diffusion processes related to the exterior Dirichlet problem is not so evident. For example, the potential field on the exterior of a charged conducting body is also governed by the solution of the exterior Dirichlet problem where the capacity governs the decay of the potential field at large distances from a charged body. Other examples are discussed below.

Most of our discussion relates to electrostatic capacity or hydrodynamic friction on bodies of general shape and occasionally we mention Smoluchowski rate constants. Before proceeding to these problems we emphasize that there are numerous other physical problems which require the calculation of the capacity. Kac and Luttinger [8], for example, showed that the low energy scattering length of an impenetrable body equals the capacity of the body [9]. The capacity is then of considerable interest in quantum theory. The far field acoustic scattering length of "soft" bodies is also proportional to the capacity of the scatterer [9(b)–9(e)], so capacity is important in acoustic applications, especially applications associated with

diffraction of sound through screens. The mutual virial coefficient between a polymer chain and a protein or other compact particle having dimensions much smaller than the polymer chain is proportional to the capacity of the compact particle and the molecular weight of the polymer chain [10]. Capacity is thus important in controlling the stability of protein solutions in the presence of polymer additives and associated applications involving protein separation [11]. The tones of resonators are related to the capacity of the holes since capacity controls the rate of flow of inviscid fluids (air to a reasonable approximation) through barrier holes [1]. The tones of imperfect clamped drums having holes cut of various shapes is related to the tone of the perfect drum and the capacity of the holes [12]. Capacity is then important in the theory of musical instruments [2]. The remarkably high rate of evaporation of water through the stomata of leaves can be understood in terms of the capacity of the stomata [13]. Numerous capacity applications involve surfaces in contact and the flow of energy in the form of heat, electricity, or the action of mechanical forces. For example, the capacity of contact points between surfaces governs the steady-state flow of heat [14] and electricity [15] between bodies in contact. Thus calculations of the capacity of complicated regions of contact between surfaces are important in the design of insulating windows [14], motor brushes, switches, and other electrical devices [15]. The grounding of high voltage power systems in particular has required a knowledge of the variation of capacity with body shape since the resistance to ground is inversely proportional to the capacity of the grounding elements [16]. There are also applications related to the shielding of electrical devices from various kinds of incident fields and the design of antennas [16,17]. The engineering literature of all these applied problems is a rich source for capacitance calculations on complicated-shaped bodies and these examples also point to further practical applications for the probabilistic method discussed below.

Models of physical processes related to the exterior Dirichlet problem naturally start with the simplest case of a spherical boundary. For example, the Smoluchowski rate constant k_s for point particles diffusing toward a stationary absorbing sphere of radius a equals [18]

$$k_s(\text{sphere})=4\pi Da \ , \tag{1.1}$$

where D is the diffusion coefficient of the particles. The steady-state "thermal capacitance" (or conductance) of a sphere at constant temperature radiating heat into the surrounding medium is described by (1.1) where D is replaced by the thermal conductivity κ [3(a),14,19,20]. The thermal capacitance describes the rate of heat flux of a heated (cooled) object into a surrounding medium having a lower (higher) temperature at distances large compared to the object size. The rate of heat transfer is evidently a functional of surface shape and the (thermal) capacitance is minimized by a sphere of all objects having finite fixed volume [1,3]. In electrostatics the capacitance of a conducting sphere, i.e., the total charge on a sphere having radius a which is maintained at unit potential with respect to infinity, equals [21]

$$C(\text{sphere})=a \ . \tag{1.2}$$

Mathematically the thermal and electrical capacitances are equivalent [19] and we just use the term "capacitance" to indicate both quantities. We also observe that the translational friction coefficient f of a sphere in a viscous fluid is proportional to the particle radius [22,23]

$$f(\text{sphere})=6\pi\eta_s a \ , \tag{1.3}$$

where η_s is the solvent viscosity. The relation between friction f and capacitance C is discussed below.

Generalization of these physical problems to objects having arbitrarily shaped boundaries leads to a consideration of the exterior Dirichlet problem in its full generality. In the generalized theory the capacity C replaces the sphere radius a as the appropriate measure of particle "size." From a formal standpoint the calculation of C simply involves the solution ϕ of Laplace's equation on the exterior of the arbitrarily shaped region where the surface boundary condition can be taken as unity without loss of generality. The decay of $\phi(\mathbf{r})$ at a large distance r from an arbitrary point on the body defines the capacity C [1,8],

$$\phi(\mathbf{r})\sim C/r+O(1/r^2), \quad r\to\infty \tag{1.4a}$$

or more concisely [24],

$$\lim_{r\to\infty}[r\phi(\mathbf{r})]\equiv C \ . \tag{1.4b}$$

There are complementary variational (Dirichlet and Thomson) principles which give variational upper and lower bounds to the capacity [1,5]. The probabilistic interpretation of C in terms of the hitting probability of random walks has also been discussed at length [7] and this approach is implemented below.

The Smoluchowski rate constant k_s for an arbitrarily shaped object then equals [25]

$$k_s=4\pi DC \ , \tag{1.5}$$

which reduces to the sphere result for $C(\text{sphere})=a$. Other properties related to the capacity follow similarly.

The relation between the friction coefficient f and the capacity C is more delicate than the other physical properties discussed above. Hubbard and Douglas [26] recently derived an approximation for the friction coefficient of an arbitrarily shaped Brownian particle [26],

$$f\approx 6\pi\eta_s C \ , \tag{1.6}$$

which generalizes the exact Stokes-Einstein result (1.3) for a sphere. The derivation of (1.6) assumes an angular averaging approximation, based on physical arguments. As in other applications of the angular averaging approximation in condensed matter physics [26], this approximation has proven to be accurate for estimating f. Indeed, Eq. (1.6) has been shown to be accurate to better than 1% in cases where exact solutions are known [26]. We caution, however, that the accuracy of the angular averaging approximation for skew-shaped bodies is not known presently, so that the approximation should not

be adopted uncritically. We expect that (1.6) should be generally accurate to within a few percent, which should be sufficient for many hydrodynamic applications. We *assume* that this approximation holds for all shapes considered. Estimates below the friction coefficient for complex shaped objects (e.g., polymer chains), based on (1.6) and our numerical estimates of C, accord to within numerical uncertainty with the best current numerical estimates of the friction coefficient obtained by alternative, more conventional, hydrodynamic methods.

We note that the "hydrodynamic radius" R_H is conventionally *defined* by an equation of the form (1.6), where R_H corresponds to C, and that (1.6) can also be employed to estimate particle capacity. Such estimates of capacity from hydrodynamic measurements should be useful in a variety of contexts.

II. PROBABILISTIC CALCULATION OF CAPACITY

The algorithm of Luty, McCammon, and Zhou [27–31] is particularly suitable for calculating the capacitance and the translational friction of arbitrarily shaped objects. In its original design the algorithm treats a general boundary condition for the probability density $p(\mathbf{r})$ of particles diffusing to an absorbing surface Ω. The algorithm for calculating Smoluchowski rate constants allows for an interaction potential $U(\mathbf{r})$ between the object and the diffusing particles, but the applications below are limited to a vanishing potential $U(\mathbf{r})=0$. The probability density of the diffusing particles at infinity is fixed at 1, and the Smoluchowski reaction rate then equals [27,29]

$$k_s = k(b)\beta_\infty \ . \tag{2.1}$$

The rate constant k_s characterizes the steady state flux across Ω (see Fig. 1), $k(b)$ is the reaction rate toward a spherical surface $r=b$ that encloses the object Ω, and β_∞ is the probability that particles which start on the "launching surface" $r=b$ will react with the "probed surface" Ω rather than escape to infinity. It is the hitting probability β_∞ that is obtained by this probabilistic method. A separate publication provides the technical details for the efficient calculation of capacity [29], since the algorithm has an independent interest from the applications developed below. The "capacitory potential" $\phi(\mathbf{r})$ is related to $p(r)$ by $\phi(\mathbf{r})=1-p(\mathbf{r})$. With this choice the potential $\phi(\mathbf{r})$ also satisfies Laplace's equation and has value 0 at infinity and 1 on the surface Ω. Since

$$C=-(4\pi)^{-1}\int_\Omega d\sigma\cdot\nabla\phi(\mathbf{r})=(4\pi)^{-1}\int_\Omega d\sigma\cdot\nabla p(\mathbf{r}) \ ,$$

$$k_s=D\int_\Omega d\sigma\cdot\nabla p(\mathbf{r}) \ ,$$

and k_s for a sphere of radius b equals $k_s(\text{sphere})=4\pi Db$, the capacity reduces to

$$C=b\beta_\infty \ . \tag{2.2}$$

To estimate β_∞ we launch Brownian particles uniformly from a spherical launching surface having radius $r=b$ [28]. When all the particles are stopped because they either hit the surface Ω or have escaped to infinity, the fraction which hits the surface first determines β_∞, the "hit fraction." From (1.5), (1.6), and (2.2) we then obtain the diffusion-controlled reaction rate k_s, the electrostatic capacitance C, and an estimate of the friction coefficient f from (1.6).

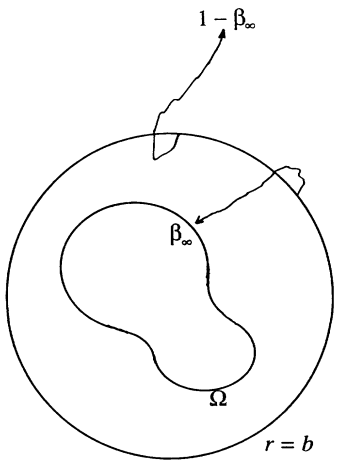

FIG. 1. A schematic illustration of the calculation of the hitting probability β_∞.

III. APPLICATIONS

The advantage of the probabilistic path method (PPM) of calculating capacitance is that it allows a general treatment of arbitrary mass distributions contained in a finite region without program modification. We simply draw our launch sphere about the set in question, launch the walks ("paths"), and collect statistics. We illustrate the versatility of the method by some examples. The first examples of a cube and intersecting spheres continue the tabulation of "blunt" bodes given by Hubbard and Douglas [26]. These calculations show that the capacity of objects having sharp boundaries can be accurately calculated by the PPM. We then treat a collection of spheres randomly distributed on a large spherical surface to illustrate the significant screening effects that arise in this geometry and the role of receptor position fluctuations on the total average reaction rate. Finally, we consider various chains of spheres placed on rod and random walk frameworks. The PPM results are compared with the Kirkwood-Riseman double sum formula for the friction of polymer chains [32,33] to estimate the configuration preaveraging errors incurred in Kirkwood's calculations and the PPM results are also compared with recent non-pre-averaging Monte Carlo calculations for the friction.

A. Cube

To illustrate the PPM algorithm in a nontrivial case we consider the capacitance of a cube which has been characterized as "one of the major unsolved problems of electrostatic theory" [34]. Consider a cube having a side of length a. This cube is closely encircled by a sphere of radius $r=(3^{1/2}+0.1)a/2$ and we adopt a time step $D\Delta t=5\times10^{-4}a^2$. We then launch 2 million particles from the enclosing sphere. The particles "rain down"

upon the cube and 1 448 023 of them ultimately hit the cube so the hit fraction β_∞ equals 1 448 023/2 000 000. From Eq. (2.2) we directly infer the capacitance,

$$C(\text{cube})=r\beta_\infty=0.663a \ . \tag{3.1a}$$

The PPM estimate agrees to within 1% of the best numerical boundary element estimate of Cochran [35]

$$C(\text{cube})/a=0.6596 \tag{3.1b}$$

and with the conjectured exact value of Hubbard and Douglas [26,36]

$$C(\text{cube})/a=(32\pi^3/\sqrt{6})/\Gamma(\tfrac{1}{24})\Gamma(\tfrac{5}{24})\Gamma(\tfrac{7}{24})\Gamma(\tfrac{11}{24})$$
$$=0.6594\ldots \ (\text{conjecture}) \ . \tag{3.1c}$$

B. Intersecting spheres

The example of two overlapping or "fused" spheres also presents an example in which the boundary exhibits a sharp edge at the point of sphere intersection. Intersecting spheres have shapes which range from "crescent" to "snowman-like" forms [37]. Calculation of the capacity of intersecting spheres is possible by classical methods. The electrostatic potential on the exterior of the touching spheres can be expressed in toroidal coordinates as [37]

$$\phi(\alpha,\beta,\varphi)=[2\sqrt{\cosh\alpha-\cos\beta}/\pi]\int_0^\infty d\tau[\sinh(\beta+\beta_0-2\pi)\tau+\sinh(2\pi+\beta_0-\beta)\tau]\frac{\cosh(\pi-\beta_0)\tau}{\sinh(\pi\tau)\sinh(2\beta_0\tau)}$$
$$\times\int_\alpha^\infty \frac{d\theta\sin\theta\tau}{\sqrt{\cosh\theta-\cosh\alpha}}, \quad 2\pi-\beta_0\le\beta\le2\pi+\beta_0 \tag{3.2}$$

where the coordinates (α,β,φ) are related to the Cartesian coordinates as given in Ref. [31] and $\cos\beta_0=l/2a$. An example of two intersecting spheres is illustrated in Fig. 2. The capacitance equals

$$C/a=-\int_0^\infty d\alpha\frac{\sin\beta\sinh\alpha}{\cosh\alpha-\cos\beta}\frac{\partial\phi}{\partial\beta}\bigg|_{\beta=2\pi-\beta_0} \ . \tag{3.3}$$

For $\beta_0=30°$ and 45°, the integral can be evaluated analytically and the results are $C/a=1.345$ and 1.293, respectively. We launched 10^4 random walks from a sphere enclosing two identical spheres separated at two intersphere distances $l/2a=\cos30°$ and cos45°. The PPM estimates of the intersecting sphere capacity then equal

$$C(\beta_0=30°)/a=1.36 \ , \tag{3.4a}$$

$$C(\beta_0=45°)/a=1.28 \ , \tag{3.4b}$$

following the procedure discussed above for the cube.

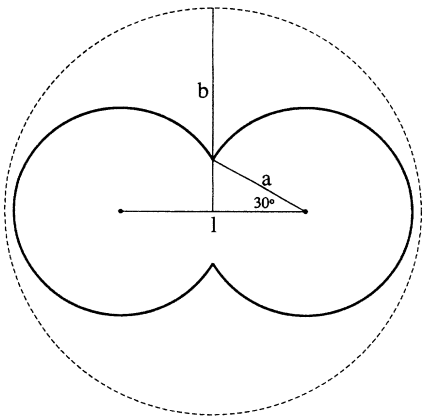

FIG. 2. Two intersecting spheres for an intersphere separation of $l/2a=\cos30°$.

These simulation estimates agree with exact results to within 1%.

For completeness we also mention the case of separated spheres of radius a which arise in the discussion below. Taking l as the separation distance between the sphere centers, we find by probabilistic simulation

$$C(l=2a)/a=1.40, \quad C(l=4a)/a=1.61 \ . \tag{3.4c}$$

These results are compared with classical analytical estimates of $C(l)$ and $f(l)$ summarized by Hubbard and Douglas [26],

$$C(l=2a)/a=1.386, \quad C(l=4a)/a=1.605 \ ; \tag{3.4d}$$

$$f(l=2a)/6\pi\eta_s a=1.392 \ ,$$
$$f(l=4a)/6\pi\eta_s a=1.605 \ . \tag{3.4e}$$

Ellipsoids subjected to Kelvin inversion constitute a class of exactly solvable blunt body forms which were not included in the summary by Hubbard and Douglas [26]. The inverted prolate ellipsoid is particularly important because it closely resembles the shape of human red blood cells and other irregularly shaped vesiclelike structures. We note the recent exact analytic calculations of Dassios and Kleinman [38] for the capacity of inverted ellipsoids.

C. Randomly distributed beads on a ball

One of the most useful methods of calculating the friction of complicated shaped bodies involves placing spherical "beads" at high density on the body surface [39,40]. This gives an increasingly accurate description of the friction, but even for the simplest shapes the procedure becomes computationally demanding [40]. Rather good friction estimates of structures with complicated shapes can be obtained if the Rotne-Prager improvement to the idealized point Oseen approximation to the finite bead friction is incorporated in these "shell model" calcula-

tions [41]. Calculations of this kind are summarized by de la Torre and Bloomfield [42]. It is emphasized that the Rotne-Prager approximation is *irrelevant* to hydrodynamic calculations which do not attempt to approximate extended bodies by effective point sources (i.e., beads). Such approximations are not involved when the PPM is employed in conjunction with (1.6) to calculate C and the scalar friction f.

We start with a spherical surface of radius R and distribute smaller spherical beads of radius $a=R/10$ randomly onto the spherical surface with a uniform distribution such that the beads are allowed to overlap. The larger spherical surface is a phantom boundary introduced simply to define the positioning of the beads in space. A PPM calculation of the arithmetic mean of 250 configurations of beads ($N=2,11,51$) gives

$$\begin{aligned} C(N=2)/a &= 1.85 , \\ C(N=11)/a &= 5.77 , \\ C(N=51)/a &= 9.15 . \end{aligned} \tag{3.5}$$

For large N the dimensionless capacitance $C(N)/a$ approaches the limiting value $C(N\to\infty)/a=11$, since the sphere becomes a dense spherical shell having an outer radius equal to $11a$ for $N\to\infty$. (A separate publication provides data for numerous values of N as an illustration of the PPM for a statistically defined object [29].) The 51 bead example lies within 17% of the large N limit, even though only about 10% of the shell is covered with beads. This "screening effect" between the beads is significant for diffusion controlled reactions and the biological importance of this effect is discussed by Berg and Purcell [13,25]. The hydrodynamic analog of this screening effect is discussed by Bloomfield, Dalton, and Van Holde [43].

The application of the standard Kirkwood-Riseman (KR) double sum (DS) friction estimates of spheres randomly distributed on a sphere gives [32,43]

$$\begin{aligned} &f(N, \text{ beads on sphere; DS}) \\ &\qquad = N\zeta_a/[1+(N-1)(N\zeta_a/\zeta_b)] , \\ &\zeta_a=6\pi\eta_s a, \quad \zeta_b=6\pi\eta_s R , \end{aligned} \tag{3.6}$$

which was obtained previously by Pastor and Zwanzig [45]. Since the KR theory involves the angular averaging approximation of the Oseen tensor, this expression can be equally considered as an approximation to the capacity of the beads on a sphere where f is simply replaced by C and ζ_a/ζ_b is replaced by a/R. The double sum estimates of the capacity for the values of N investigated above are equal,

$$\begin{aligned} C(N=2;\ \text{DS})/a &= 1.83 , \\ C(N=11;\ \text{DS})/a &= 5.54 , \\ C(N=51;\ \text{DS})/a &= 8.51 . \end{aligned} \tag{3.7}$$

We notice a significant discrepancy between the DS and PPM estimates for $N=51$ beads. This effect is due to the configurational preaveraging approximation which neglects fluctuations in the sphere configurations. The effect of such fluctuations is less when the surface coverage is high or low [29].

A variation of the beads on a sphere calculation has also been given by Berg and Purcell [25] for the rate of diffusion controlled ligand binding to N randomly distributed disk-like receptors of radius a on a sphere of radius R. The Smoluchowski rate constant k_s is calculated approximately as [25]

$$k_s = Nk_{\text{disk}}/[1+(N-1)k_{\text{disk}}/k_{\text{sphere}}] , \tag{3.8a}$$

$$k_{\text{disk}}=4Da, \quad k_{\text{sphere}}=4\pi DR . \tag{3.8b}$$

From (1.5) the capacitance analog of this expression equals

$$\begin{aligned} &C(\text{disks on a sphere}) \\ &\qquad = NC_{\text{disk}}/[1+(N-1)C_{\text{disk}}/C_{\text{sphere}}] . \end{aligned} \tag{3.9}$$

The Berg-Purcell [25] estimate of the Smoluchowski rate constant evidently employs a preaveraging approximation similar to the KR hydrodynamic theory. We note that (3.9) exactly corresponds to (3.6) where the bead capacity (or friction) replaces the disk capacity. This suggests the general approximation

$$C(N)\approx NC/[1+(N-1)C/C_{\text{sphere}}], \quad C_{\text{sphere}}=R \tag{3.10}$$

for compact particles of arbitrary shape having capacity C distributed at random on a sphere. This expression can be applied to a variety of contexts to estimate (roughly) the friction f, the rate constant k_s, and the capacity C when the absorbers have a specifically known structure. Goldstein and Wiegel derived the estimate (3.10) for the case of hemispheres on a large reflecting sphere [25(c)].

The configuration preaveraging approximation makes the accuracy of the Kirkwood-Burg-Purcell–type estimate [Eq. (3.10)] somewhat uncertain. Recently, Northrup studied the role of receptor fluctuations on the capacity in the case of N circular "receptors" on a sphere to test the original Berg-Purcell mean-field ("independent receptor") calculation [46,47]. Northrop's calculation shows that the mean-field estimate of C for the patched sphere [(3.10)] is consistently lower than the simulated result which accounts for fluctuations in the patch configurations. This result accords well with the results mentioned above for beads on a sphere. For $N=50$ receptor disks of radius $a\approx R/16$ the preaveraging error is about 5%, compared with the nearly 4% discrepancy mentioned above for $N=11$ beads on a sphere. Fluctuations in the configuration of the receptors leads to a significant increase in the rate constant k_s from what might be expected from a "typical" receptor configuration because of the large contribution of rare more symmetric configurations having significantly higher capacity [47]. This same effect arises in configurations of beads situated on the vertices of a random walk, but the effect is intensified because the density of the beads does not become uniform as $N\to\infty$. Fluctuations are always large in random walk chains due to the tendency of the backbone of the typical random walk path to drift away from the position of its endpoint.

D. Chains of spheres

For many years the hydrodynamic properties of polymer chains have been modeled using the "pearl necklace" model of beads strung along a volumeless and frictionless filament [48–51]. There are variations in which the filament is "springlike," a rigid phantom rod, or a tethered flexible string. The basic "beads on a string" picture, however, is invariant. The earliest calculations by Kramers [49], Debye [50], and Rouse [51] neglected the hydrodynamic interactions and these interactions were emphasized in later calculations by Kirkwood and Riseman [32] and many others following their pioneering work. Recent contributions have emphasized the configuration preaveraging approximation which introduces significant errors into mean-field calculations of polymer friction and other hydrodynamic properties. Since the PPM does not employ the configurational preaveraging approximation it is interesting to compare these calculations of polymer friction (capacity) with recent non-pre-averaged hydrodynamic calculations and with analytic (but perturbative) renormalization group calculations.

1. Linear chain of spheres

The simplest example of a chain of spheres involves placing spheres at a constant intersphere spacing along a line. As in the example discussed above, we denote the distance between the two neighboring sphere centers by l and give this distance in units of the sphere (bead) radius a. In Table I we tabulate the capacitance of a linear array of spheres obtained by the probabilistic method at two intersphere separations $4a$ and $2a$. The error estimates indicated in Table I are discussed in Ref. [29]. For reference we calculate the (mean-field) double sum estimate [32] of KR for the translational friction f,

$$f(\mathrm{KR,\ double\ sum})=N\zeta_a \Big/ \left[1+\left[\sum_i \sum_j a/r_{ij}\right]\Big/N\right], \quad i\neq j \tag{3.11a}$$

where r_{ij} is the average interbead distance $|i-j|l$. Discrete integration gives

TABLE I. Capacitance of a linear rodlike array of spherical beads.

	$l/a=4$		$l/a=2$	
N	C(PPM)/a	C(DS)/a	C(PPM)/a	C(DS)/a
2	1.614±0.015	1.600	1.396±0.009	1.333
5	3.089±0.043	3.046	2.294±0.025	2.190
10	5.093±0.085	5.090	3.595±0.048	3.414
17	7.886±0.142	7.658	5.366±0.080	4.942
26	11.04±0.21	10.71	7.067±0.105	6.486
37	14.25±0.29	14.23	9.582±0.163	8.806
50	18.50±0.38	18.18	11.33±0.21	11.11
65	23.36±0.50	22.57	14.35±0.27	13.66
82	28.76±0.63	27.38	17.26±0.34	16.43
101	32.75±0.74	32.59	19.93±0.40	19.43
401	107.0±2.7	105.9	64.84±1.49	61.01

$$f(\mathrm{KR;\ double\ sum})=N\zeta_a/\{1+[\psi(N+1)-1+\gamma]N\zeta_a/\zeta_{\mathrm{rod}}\}, \tag{3.11b}$$

$$\zeta_{\mathrm{rod}}\equiv 6\pi\eta_s(Nl/2), \tag{3.11c}$$

where $\psi(x)=\Gamma'(x)/\Gamma(x)$ is the psi function and γ is Euler's constant. Equation (3.11a) can be equally regarded as a mean-field approximation for the capacity. A comparison of the simulation results for the linear chain of spheres and the KR double sum estimates shows that the deviation is rather constant for a given bead separation. For $l=4a$ and $2a$ the discrepancy is about 1–2% and 4–6%, respectively. These deviations are comparable with the error which exists between the KR expression for $N=2$ and the exact results mentioned above [52]. This relative constancy of the deviation between the simulation and the DS estimates is natural given the very weak screening in the rod configuration. In the complete absence of screening $f(C)$ is proportional to the number of beads and (3.11) gives a slight correction $\psi(N+1)-1+\gamma$, which describes the screening for the linear bead array. We conjecture that the linear bead array in $d=3$ has the maximum capacity of all arrays having linear chain topology. A sphere is known to maximize the capacity of objects of a given volume, but the addition of auxiliary shapes makes other shapes extremize the capacity [1]. Knowledge of the capacity extremes is important in modeling fluctuations in C (or f) in flexible polymer chains. We next consider this more interesting case.

2. Gaussian chain of overlapping spheres

The Gaussian chain model is a standard model of flexible polymer chains. In this model the bond vector distance $r_{ij}=|\mathbf{r}_i-\mathbf{r}_j|$ is chosen to have a Gaussian distribution [33]

$$\tau(r_{ij})=(2\pi l^2/3)^{-3/2}\exp[-3(r_{ij})^2/2l^2], \tag{3.12}$$

where l is the root-mean-square bond length. First, we placed spheres having radius a at the vertices of a Monte Carlo generated chain and we then launched 10^3 random walks from a spherical surface enclosing each chain configuration. The capacitances for various a/l values, averaged over 250 configurations of chains of 26 and 101 spheres, are shown in Table II. The capacitances for both $N=26$ and 101 can be well reproduced by a function of the form

$$C=\frac{Na}{1+c_1(1-c_2a/l)(N-1)^{1/2}a/l}. \tag{3.13}$$

For $N=26$ the constants are $c_1=2.872$ and $c_2=0.493$ and for $N=101$ they are 3.109 and 0.383, respectively.

We note for reference in the discussion below that the radius of gyration $\langle S^2\rangle_0^{1/2}$ for a Gaussian chain equals

$$\langle S^2\rangle_0=(N-N^{-1})/6. \tag{3.14}$$

The Kirkwood-Riseman (DS) estimate [32] of the friction (capacity) is also included in Table II for comparison. In this case we observe very significant discrepan-

cies between the simulation and the mean-field DS estimates. For $N=101$ and $2a/l=2$ we find a significant 17% deviation. This discrepancy is usually discussed in terms of the measurable ratio $R_H/\langle S^2\rangle^{1/2}\equiv\psi_H$, where R_H is the hydrodynamic radius (as mentioned in the introduction R_H equals C in the angular averaging approximation). This ratio for the Gaussian chain model ($N=101$) is shown in Fig. 3 as a function of the bead-bond length ratio. The solid line interpolates the simulation results in the angular average approximation and the dashed line denotes the Kirkwood-Riseman DS estimate. Observe that the discrepancy between the simulation and DS estimates grows significantly with increasing a/l. Clearly, the error approaches zero in the limit $a/l\to 0^+$. Fluctuation errors are generally small when the hydrodynamic interactions are weak as in the rod array discussed above.

Previous estimates of the preaveraging error in rigid pearl necklace models of polymer chains have conventionally chosen [53] $a/l\approx\frac{1}{4}$ or a slightly larger value [54] $a/l\approx 0.271$ since these choices seem to reproduce limiting $N\to\infty$ results in simulations of modest chain length [53]. Interestingly, a similar "special" ratio $a/l\approx\frac{5}{18}\approx 0.278$ is commonly invoked to "optimally" model excluded volume interactions in bead models of excluded volume interactions in polymers [54]. In Fig. 3 we obtain $\psi_H(\mathrm{DS})=0.684$ for $a/l\approx\frac{1}{4}$, which accords rather well with the infinite chain length estimate $\psi_H(\mathrm{DS},N\to\infty)=3\pi^{1/2}/8=0.667$, expected from the continuum limit infinite chain Kirkwood-Riseman calculation [32,33]. The PPM estimate for ψ_H for $a/l=\frac{1}{4}$ equals $\psi_H(\mathrm{PPM})=0.771$, which is 11% larger than the DS estimate. The simulation result is consistent with Zimm's calculations, which indicate a 12% deviation of ψ_H from the Kirkwood-Riseman DS value for a 51 bead chain with $a/l=0.271$ [53]. Zimm directly treats the rigid body Kirkwood-Riseman equations without configurational preaveraging using a Monte Carlo (MC) method. This technique is quite independent from our probabilistic method. More extensive MC calculations of the preaveraging approximation for pearl necklace models of freely jointed polymer chains without excluded volume ($a/l\approx 0.25$) by de la Torre and co-workers [54] confirm the original estimate of Zimm to be a good approximation.

TABLE II. Capacitance C of Gaussian chains of overlapping spherical beads.

	$N=26$		$N=101$	
a/l	C(PPM)/a	C(DS)/a	C(PPM)/a	C(DS)/a
0.0630	13.85±1.41	13.57	34.40±3.51	33.15
0.0945			26.18±2.99	24.87
0.116			22.72±2.63	21.19
0.126	9.531±0.946	9.232	21.52±2.35	19.91
0.131			20.80±2.32	19.27
0.150			18.81±2.17	17.27
0.165			17.43±1.96	15.96
0.189	7.491±0.854	7.027		
0.233	6.604±0.801	6.040		
0.250			12.66±1.44	11.23
0.252	6.328±0.696	5.698		
0.263	6.090±0.738	5.526		
0.300	5.568±0.678	4.989		
0.331	5.239±0.609	4.637		
0.500	4.007±0.468	3.384	7.395±0.884	6.116

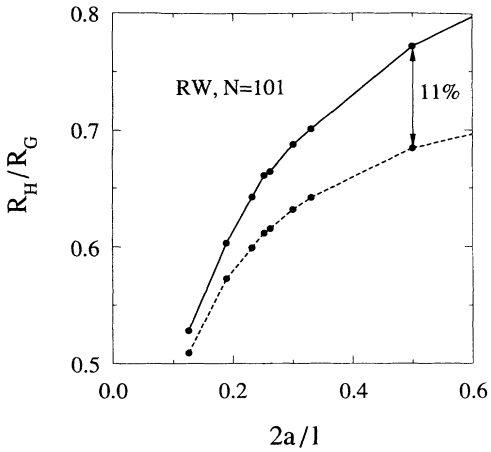

FIG. 3. Dimensionless ratio $\psi_H=R_H/R_G$ for Gaussian chains of overlapping beads. The lower dashed curve is an interpolation of the preaveraging results of Kirkwood and Riseman [32] and the solid line interpolates between PPM estimates.

Experimental estimates of ψ_H in theta solvents (polymer solutions for which the second virial coefficient vanishes) are often found in the range [55] (0.77,0.79), which is consistent with the simulation estimate for a Gaussian chain $\psi_H(\mathrm{Gaussian})=0.771$. The alternative MC calculations, following the more traditional type of hydrodynamic calculations [53,54], also accord rather well with experiment and the PPM calculations.

Although the agreement with experiment is encouraging, Fixman [56] has provided evidence that the dynamic flexibility ("internal viscosity") of the chain can appreciably affect ψ_H so that the rigid body value of ψ_H should only be an upper bound. By allowing the rare extended chain configurations, which give rise to the enhanced friction (capacity), to relax at a rapid rate the mean-field hydrodynamic theory of KR becomes a better approximation. (This observation obviously has implications for the corresponding problem of mobile absorbing sites in the sphere-receptor problem [25].) It also should be appreciated that the Gaussian chain model is an idealization for theta point polymers and that ternary interactions can lead to appreciable contributions to ψ_H [57]. Other complicating factors in estimating ψ_H are summarized by Wang, Douglas, and Freed [44] and Douglas and co-workers [58]. Configurational preaveraging, however, remains the largest factor which limits the development of a quantitative theory of polymer solution hydrodynamics (capacity).

3. *Nonoverlapping (self-avoiding) spheres on a random walk string*

The Gaussian chain of overlapping spheres model is a rather idealized model of real polymer chains which ex-

hibit excluded volume interferences between the chain elements and attractive short range interactions. The application of the Gaussian chain model is limited to the theta temperature where the excluded volume and attractive interaction effects largely compensate [33]. In a temperature range where the polymer chain swells the excluded volume forces predominate and it then becomes necessary to enforce the nonoverlapping condition so that the simple Gaussian chain model is no longer adequate. To take this effect into account we searched through the configurations of a Gaussian chain, generated as described in Sec. III D 2, and selected those in which no spheres overlapped. The radius of gyration $\langle S^2\rangle^{1/2}$, calculated by averaging over 10^4 such configurations, is shown in Table III for a chain of 26 nonoverlapping spheres at various a/l values. We than launched 10^3 random walk particles from a spherical surface enclosing each chain configuration. The capacitances for various a/l values, averaged over 250 configurations of the chain of 26 nonoverlapping spheres, are given in Table III along with the Kirkwood-Riseman DS estimate for comparison.

The ratio ψ_H for the self-avoiding beads indicates some interesting effects. First of all, we observe in Fig. 4 that the DS value of ψ_H(DS;SAW)=0.667 is only slightly different (less than 3% change) than the value of ψ_H(DS) in the *absence* of self-avoidance. Renormalization group (RG) calculations of the configurational *preaveraged* KR theory with excluded volume interactions indicate that the change of ψ_H(DS) with and without preaveraging should be less than 1% [59,60]. The simulation results then accord well with the expectations of these analytic RG calculations. Another striking feature is that the preaveraging error indicated by the PPM simulations is *smaller* for the self-avoiding walk (SAW) than for Gaussian overlapping sphere chains with the same a/l ratios. For the conventional ratio $a/l\approx\frac{1}{4}$ the error for the self-avoiding chains is only about 5% rather than the 11% discrepancy found for overlapping chains. (The chain lengths differ, but this does not account for the large discrepancy.) This finding is rather sensible since the chains become more extended with excluded volume interactions and the preaveraging errors decrease because of the diminished screening with swelling. Second order in $\epsilon=4-d$ dynamical renormalization group calculations by Wang, Douglas, and Freed [44] accord qualitatively with these findings and predict that ψ_H preaveraging

TABLE III. Radius of gyration and capacitance of a self-avoiding chain of spherical beads.

a/l	$\langle S^2\rangle/l^2$	C(PPM)/a	C(DS)/a
0.0630	4.384	13.94±1.32	13.66
0.126	4.777	10.00±0.90	9.611
0.189	5.606	8.235±0.796	7.838
0.233	6.375	7.516±0.733	7.139
0.252	6.778	7.282±0.704	6.893
0.263	7.023	7.164±0.664	6.829
0.300	7.950	6.838±0.630	6.466
0.331	8.719	6.605±0.561	6.249

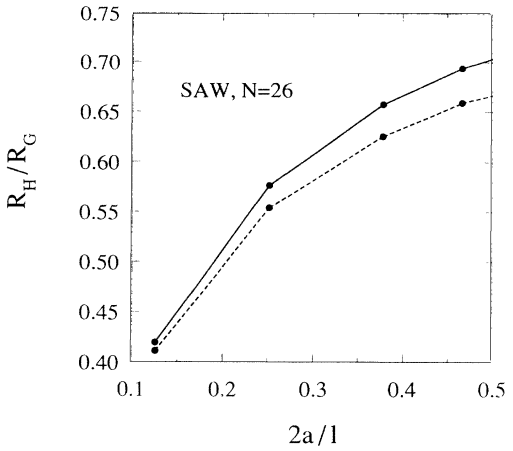

FIG. 4. Dimensionless ratio $\psi_H=R_H/R_G$ for Gaussian chains of nonoverlapping beads on a random coil chain. The lower dashed curve denotes the preaveraging (DS) calculations of Kirkwood and Riseman [32] and the solid line interprolates between PPM estimates.

corrections should be nearly twice as large for continuum Gaussian chains than for self-avoiding chains. Unfortunately, the magnitudes of the preaveraging errors predicted by RG theory are too large by a factor of about $\frac{5}{2}$. The main problem is that the perturbative expansion parameter $(4-d)/4$ of the hydrodynamic theory is not small in $d=3$ spatial dimensions so that the ϵ-expansion perturbative theory is not as useful as in other applications (e.g., polymer excluded volume).

We also observe that the simulation estimate of ψ_H for self-avoiding and Gaussian chains equals ψ_H(SAW)/ψ_H(Gaussian)$\approx$0.91 for $a/l\approx\frac{1}{4}$. In the polymer literature this ratio is often denoted the "Flory constant" ratio [33,38] P^*/P_0. Recent Monte Carlo estimates of P^*/P_0 for rigid freely jointed chains in the absence of configurational preaveraging by Bernal *et al.* [61] indicate $p^*/P_0=0.92$ for $N=80$, in accord with our simulation estimate. These calculations (analytic and numerical) indicate that the largest contribution to the excluded volume dependence of dimensionless ratios such as P^*/P_0 derives from the *excluded volume dependence of hydrodynamic fluctuations,* i.e., the preaveraging errors are dependent on the excluded volume interaction. Since there is no quantitative method for performing analytic calculations of hydrodynamic properties in the absence of preaveraging (even in the absence of excluded volume interactions), we must conclude that the presently available analytic theory of polymer chain dynamics is rather inadequate. The probabilistic path method is especially valuable under these circumstances.

For temperatures below the theta point the attractive interactions predominate so that flexible chains coil into a compact "spongelike" configuration. The friction (and capacity) is highly screened in this type of compact configuration and f and C approach $M^{(d-2)/d}$ scaling in the limit of very strong attractive interactions where M is the chain mass. The $M^{(d-2)/d}$ scaling for $d>2$ is a

rigorous lower bound for the scaling of capacity with mass [7(e)]. The Smoluchowski rate constant for the polymeric chain of absorbers evidently undergoes a steep drop as the chains "collapse" into a compact state below the theta temperature. In other instances the capacity (rate constant) may greatly increase with a polymer conformational transition. For example, when polymers absorb onto surfaces the chains tend to spread out due to increased excluded volume interactions in the adsorbed state and the capacity thus greatly increases. The Smoluchowski rate constant for a polymeric chain of receptors exhibits great variability as a function of chain conformation [33]. Chain conformation in turn is influenced by chain environment.

IV. CAPACITY, FRICTION, AND FLUCTUATIONS OF THE "WIENER SAUSAGE"

The capacitance of an arbitrarily shaped particle can be understood from a very simple alternative geometrical point of view which complements the probabilistic path averaging method considered in the main body of the paper. Capacitance can also be interpreted in terms of the volume V_N swept out per unit "time" N by a spatially extended Brownian particle [8,26]. In other words, a particle undergoing Brownian motion sweeps out a volume ("Wiener sausage") that increases in a simple additive fashion with time N after transients die away. A Brownian particle spends a significant time visiting regions previously visited so that the limiting increase of "sausage" volume is a nontrivial functional of particle shape. Spitzer's fundamental ergodic theorem for the increase of the sausage volume indicates the universal asymptotic behavior [18,19]

$$\lim_{N\to\infty} \langle V_N \rangle / N \to 2\pi C \ , \tag{4.1}$$

where C is the capacity of the diffusing particle and $\langle\ \rangle$ denotes averaging with respect to Brownian motion paths (Wiener measure). However, it is well known that the random variable V_N exhibits large fluctuations [Eq. (4.1) suggests that the V_N fluctuations are closely related to fluctuations in the capacity of the individual chain configurations]. Specifically, the variance $\sigma^2 = \langle V_N^2 \rangle - \langle V_N \rangle^2$ of V_N increases strongly with chain length below $d=4$ dimensions and σ^2/N diverges for large N in $d=3$ [63],

$$\lim(\sigma^2/N) \sim \ln N, \quad N \to \infty \ . \tag{4.2}$$

Above four dimensions the V_N fluctuations exhibit a more normal behavior [63] $\sigma^2/N \sim$ const. The strong fluctuations in V_N reflects itself in a breakdown of mean-field theory. This effect is nicely illustrated by the celebrated limit theorem of Donsker and Varadhan [64] for $d=3$,

$$\lim_{N\to\infty} \langle \exp(-V_N) \rangle \sim \exp[-\lambda_\delta N^{3/5}], \quad N \to \infty \tag{4.3a}$$

where λ_δ is a specified constant [63]. The problem here is that the random variable $\exp(-V_N)$ places greater weight on paths for which V_N is small (i.e., paths "localized" to finite regions of space). The mean-field approximation amounts to replacing V_N by its mean or "typical" value $\langle V_N \rangle$,

$$\langle \exp(-V_N) \rangle \approx \exp(-\langle V_N \rangle) \sim \exp(-2\pi C N), \quad N \to \infty \tag{4.3b}$$

which is the "Rosenstock approximation" [65] in the analog case of lattice random walks. Clearly, a mean-field description is incorrect as $N \to \infty$. Extreme rather than typical configurations dominate the average in (4.3a).

The sausage construction for calculating capacity is also helpful in calculating transients from the steady-state capacity. Estimation of transients requires the solution of the Dirichlet problem for the diffusion equation on the exterior of the object rather than Laplace's equation [19,66]. The capacity is the steady-state rate of the diffusive flux $E(N)$ and Spitzer showed that the leading order transient to $E(N)$ for arbitrarily shaped bodies equals [19] ("Spitzer's formula")

$$E(N) \sim (2\pi C)N + 4(2\pi)^{-3/2}(2\pi C)^2 N^{1/2} + O(1) \ , \tag{4.4}$$

where C is the capacity. The "sausage volume" $\langle V_N \rangle$ is equivalent mathematically [8] to $E(N)$, which gives a rather curious geometrical interpretation of heat flow and other diffusion-limited fluxes. We should note that Spitzer's formula has been considerably extended to general random walks (Lévy flights), to variable spatial dimensionality, and the asymptotic expansion (4.4) is known through fourth order [67].

We also comment on a relation between (4.4) and the problem of excluded volume in flexible chain polymers. The coefficient 4 in the second term corresponds to the expectation of the number of binary random walk intersections. In general dimensionality ($d>2$) this coefficient equals [67,68] $1/\phi(1-\phi)$, where the "fluctuation exponent" of N equals $\phi=(4-d)/2$. It is rather curious that the critical dimension of four arises in this context. This property of the fluctuations must be related to the vanishing of the capacity of a Brownian path in $d=4$ and higher dimensions [69]. In physical terms this connection comes about because the "intersection volume" equals the "total volume" swept out by a particle, without regard to previous history of spatial occupation, minus the "sausage volume." For $d>3$ the predominant class of intersections should be binary intersections. These properties can be shown on a lattice where the number of distinct sites visited is the analog of the Weiner sausage volume [7(b),19(a)] and the number of chain steps taken is the analog of the total volume without regard to the previous history of occupation.

The transients of the Smoluchowski rate constant k_s are obtained by taking the derivative of $E(N)$ with respect to N and replacing N by the more conventional t variable. This leads to a time dependent rate $k_s(t)$,

$$k_s(t)/4\pi D = C[1 + (D\pi)^{-1/2} C t^{-1/2} + O(t^{-3/2})] \ ,$$
$$C = k_s(t \to \infty)/4\pi D \ , \tag{4.5}$$

where D is the diffusion coefficient. Spitzer's formula

(4.4) employs the convention $D=\frac{1}{2}$, but the variable D is restored in (4.5). In electrochemical [70] and reaction kinetics applications [25] the absorbing object is often considered to be embedded in a nonconducting or nonreacting plane (i.e., "reflecting" or "Neumann" boundary condition) which reduces the flux to the object by a symmetry factor of $\frac{1}{2}$ if the flux arrives from only one side of the plane. Note that the leading transient is quadratic in the capacity so these fluctuation terms are sensitive to particle shape. The particular case of current fluctuations from a disc electrode is discussed by Shoup and Szabo [70(b)].

The transients for the translational friction are also interesting and recent experiments have focused on measuring the "long time tails" associated with these transients. We observe that the time-dependent friction $f(t)$ on a sphere instantaneously brought into uniform motion equals [71] ($d=3$)

$$f(t)/6\pi\eta_s = R\,[1+(\nu_{\rm kin}\pi)^{-1/2}Rt^{-1/2}+O(t^{-3/2})]\ , \qquad t\to\infty \qquad (4.6a)$$

which reduces to the "time-dependent capacity" of a sphere $C(t)$,

$$C(t)=k_s(t)/4\pi D = f(t)/6\pi\eta_s = \frac{1}{2\pi}\frac{d\langle V_t\rangle}{dt} = \frac{1}{2\pi}\frac{dE(t)}{dt}\ , \qquad (4.6b)$$

where the kinematic viscosity $\nu_{\rm kin}$ (i.e., the diffusion coefficient of the vorticity) is equated to the diffusion coefficient in (4.5). We thus *conjecture* that the translational friction transient of an arbitrarily shaped Brownian particle impulsively brought into uniform motion *approximately* equals [see (1.6) and Ref. [26]]

$$f(t)/6\pi\eta_s \approx C\,[1+(\nu_{\rm kin}\pi)^{-1/2}Ct^{-1/2}+O(t^{-3/2})]\ , \qquad t\to\infty \qquad (4.7)$$

The transient ("skin") friction of a long rod or extended plate, which is impulsively brought into uniform motion along a direction in which the body is highly extended, is *exactly* related (slow flow limit where inertial terms are neglected) to the transient diffusive flux (capacity) to a line or plate, respectively, where the diffusion coefficient is $\nu_{\rm kin}$ in the hydrodynamic "analog" problem. This analogy between transient "heat flow" and friction transients for these geometries is discussed by Levine [72], Batchelor [73], and Rayleigh [74]. We view the conjectural result (4.7) as a natural generalization of these well known results for "large" objects (theoretically infinite extent) to objects of finite extent. It should be possible to check the *approximation* (4.7) using dynamic light scattering on suspensions of particles having well characterized geometrical shapes.

The transient in (4.6a) and (4.7) is sometimes called the "Boussinesq-Basset" contribution to the friction [71]. There is also a "virtual mass" (inertial) transient, which is discussed in the next section, which is important for accelerated particle motions and when pressure gradients exist in solutions.

V. DISCUSSION

In the present paper we calculate the capacities C of a variety of objects using a probabilistic method originally developed for the calculation of diffusion-controlled reaction rates. The Hubbard-Douglas approximation ($f\approx 6\pi\eta_s C$) also allows for an estimate of the translational friction coefficient f. We apply the probabilistic simulation method to nontrivial shaped bodies (cube, intersecting spheres) where accurate estimates are available and to more complex bodies where calculation is necessarily numerical (spheres randomly distributed on a spherical surface, spheres positioned at the vertices of a random walk with a Gaussian step distribution function with or without excluded volume interactions enforced). The polymer simulations show that the *configurational* (not angular) preaveraging approximation errors are significantly less for self-avoiding chains than for random walk bead chains because of the decreased screening with swelling. Results obtained by our probabilistic method for rigid random walk chains in conjunction with Eq. (1.6) are consistent with numerical estimates of the scalar friction by Zimm [53] and de la Torre and co-workers [54] using similar bead models of polymer chains, but very different methods for calculating the friction. An accurate analytic calculation of the fluctuations in the capacity (friction) of rigid random coil polymers and other statistically defined objects requires a better description of the fluctuations in the capacity associated with relatively rare chain configurations that can give a significant weight to the correct configurational average [47]. Mean-field-type calculations such as those of Kirkwood and Riseman [32] and Debye and Bueche [62] for polymer hydrodynamics implicitly assume such fluctuations are small so that the polymer chains can be modeled as effective spheres having dimensions on the order of the average chain radius of gyration. Similarly, the classical "receptors on a sphere" ligand binding model of Berg and Purcell [25] neglects fluctuations of the receptor configurations which can significantly increase the binding rate constant if the binding sites are fixed ("quenched") in position on the sphere surface [4].

In Sec V we consider an alternative method for calculating capacity which exploits an ergodic theorem relating to the volume swept out by a Brownian particle. This point of view not only gives insight into the fluctuation effects which limit the accuracy of mean-field polymer hydrodynamic calculations, but also provides a separate probabilistic method for estimating capacity. There is apparently no explicit algorithm implementing this approach, although Barrett and Benesch [75] have considered a closely related problem of the "total excluded volume of a Pearson walk" having beads placed at the vertices of the random walk. Fluctuation corrections to the steady-state capacity and related properties can be

calculated from the fluctuations in the approach of the sausage volume per unit time to its fixed-point value at long times. We argue that friction transients and associated long time tails can be understood from this geometrical viewpoint.

As a final point we mention that the rotational friction coefficient can be related to capacity in certain cases. For example, the rotational friction of an axisymmetric body rotating about the axis of symmetry is proportional to the capacity of the body in $d+2$ dimensions. In the extension to higher dimensions we simply rotate the body into the two "extra" dimensions so that the three-dimensional object can be thought of as a "cross section" within the higher-dimensional space. We summarize the d-dimensional results for the (angularly averaging approximation [26]) translational friction coefficient f_T and an exact result for the rotational friction coefficient f_R(axisym.),

$$f_T \approx [2d/(d-1)][H(d)/2]C(d)\eta_s \ , \tag{5.1}$$

$$f_R(\text{axisym.}) = (2/\pi)[H(d+2)/2]C(d+2)\eta_s \ , \tag{5.2}$$

$$H(d) = 4\pi^{d/2}/\Gamma(d/2-1), \quad H(d=3)/2 = 2\pi \ , \tag{5.3}$$

where Γ denotes the gamma function. The ubiquitous factor $[H(d)/2]$ is the norming constant for the free space Green's function of $\nabla^2/2$. The derivation of (4.9), which will be developed elsewhere, exploits a relation between the capacity of an axisymmetric body in $d+2$ dimensions and the virtual mass component along the symmetry axis and volume of the body in d dimensions [76,77]. The virtual mass determines the effective hydrodynamic mass under nonsteady motions (acceleration and deceleration) and thus is another parameter which is important in calculating frictional transients [1,3,5,78]. Calculation of the virtual mass involves solving Laplace's equation with a modified boundary condition [1], so that virtual mass is then just another variety of "capacity." A probabilistic calculation of the virtual mass should also be possible from an averaging over random walk paths.

The conjectured relation between friction and capacity transients [Eq. (4.7)] would similarly imply that the $t^{1-d/2}$ transients of the translational friction would be replaced by $t^{-d/2}$ for the transients of the rotational friction of axisymmetric bodies. Explicit calculation of the rotational friction of certain axisymmetric bodies (sphere and dumbbell) indeed gives a $t^{-3/2}$ decay in $d=3$ for the rotational friction transients as expected [79]. The extension of the fundamental "Spitzer formula" (4.4) to describe rotational friction transients therefore seems promising. An extension of the probabilistic potential theory approach and the associated probabilistic simulations to describe intrinsic viscosity would be very helpful in the physical characterization of irregularly shaped bodies.

[1] G. Pólya and G. Szegö, *Isoperimetric Inequalities in Mathematical Physics,* Annals of Mathematical Studies (Princeton University Press, Princeton, 1951). G. Szegö, Bull. Am. Math. Soc. **51**, 325 (1945). G. Szegö, Math. Z. **31**, 583 (1930).

[2] J. W. S. Rayleigh, *Theory of Sound, Vol. 2* (Dover, New York, 1945), p. 175, Secs. 304–306. Rayleigh showed that the flux of a invicid fluid pumped through a screen is determined by the capacity of the holes. H. Hasimoto [J. Phys. Soc. Jpn. **13**, 633 (1958)] showed that the corresponding flux for a viscous fluid is governed by the virtual mass of the holes. A recent discussion of Rayleigh's approach to flow through screens is given by E. O. Tuck [Adv. Appl. Mech. **14**, 89 (1974)].

[3] (a) G. Pólya, Am. Math. Mon. **54**, 201 (1947); (b) Q. Appl. Math. **6**, 267 (1948); (c) Proc. Natl. Acad. Sci. **33**, 218 (1947); (d) G. Szegö and G. Pólya, Am. J. Math. **68**, 1 (1945).

[4] These units correspond to a sphere of unit radius having capacity equal 1.

[5] M. Schiffer and G. Szegö, Trans. Am. Math. Soc. **67**, 130 (1949); M. Schiffer, Bull. Am. Math. Soc. **60**, 303 (1954); P. R. Garabedian and M. Schiffer, J. D'Anal. Math. **2**, 281 (1952); G. Dassios and R. E. Kleinman, Soc. Ind. Appl. Math. Rev. **31**, 565 (1989).

[6] W. R. Smythe, *Static and Dynamic Electricity* (McGraw-Hill, New York, 1950).

[7] (a) G. A. Hunt, Trans. Am. Math. Soc. **81**, 294 (1956); (b) P. Erdös and S. J. Taylor, Acta Math. Acad. Sci. Hung. **11**, 137 (1960); (c) K. Ito and H. P. McKean, J. Math. **4**, 119 (1960); (d) Z. Ciesielski, Bull. Acad. Polon. Sci., Math., Astron. Phys. **12**, 265 (1964). (e) R. A. Doney, Z. Whar. **4**, 253 (1965). (f) S. C. Port, Ann. Math. Stat. **38**, 1021 (1967). (g) K. L. Chung, Ann. Inst. Fourier **23**, 313 (1973). The interpretation of capacity in terms of "hitting" objects with random walk paths has been known in the mathematics literature for about 50 years.

[8] M. Kac, Rocky Mt. J. Math. **4**, 3 (1974). J. M. Luttinger, J. Stat. Phys. **15**, 215 (1976).

[9] (a) The equivalence between scattering length and capacity implies an equivalence between scattering length and translational friction in the angular averaging approximation [26]. R. Zwanzig and A. K. Harrison [J. Chem. Phys. **83**, 5861 (1985)] previously made physical arguments for a relationship between the friction coefficient and a scattering length; (b) J. Van Bladel, J. Sound Vib. **6**, 386 (1967); **8**, 186 (1968); J. Acoust. Soc. **44**, 1070 (1968); (c) T. B. Senior, *ibid.* **111**, 742 (1973); (d) D. S. Jones, Proc. R. Soc. Edinburgh Sect. A **83**, 245 (1979); (e) V. I. Fabrikant, J. Sound Vib. **111**, 489 (1986); **121**, 1 (1988).

[10] J. Hermans, J. Chem. Phys. **77**, 2193 (1982), considers the case where the compact particle is a sphere; J. J. Hermans and J. Hermans, J. Polym. Sci. **22**, 279 (1984); The volume excluded to a polymer (Gaussian chain) by a compact particle (e.g., sphere) equals the volume of the "Wiener sausage" formed by taking the union of sets obtained by sweeping the particle along the chain trajectory [8]. A fundamental theorem of Spitzer [19] indicates that this "sausage volume" is proportional to the capacity of the particle times the chain length (molecular weight). The proportionality of the mutual virial coefficient to chain length should be independent of excluded volume interactions within the polymer chain.

[11] D. H. Atha and K. C. Ingham, J. Biol. Chem. **256**, 12 108 (1981).

[12] S. Ozawa, J. Fac. Sci. Univ. Tokyo Sect. 1A Math. **30**, 53

(1981); R. Figari, E. Orlandi, and S. Teta, J. Stat. Phys. **41**, 465 (1985).

[13] M. Brown and F. Escombe, Philos. Trans. R. Soc. London Ser. B **193**, 233 (1900); C. S. Patlak, Bull. Math. Biophys. **21**, 129 (1959); P. Brunn, V. I. Fabrikant, and T. S. Sankar, Q. J. Mech. Appl. Math. **37**, 311 (1984).

[14] R. E. Collins, L. Poladian, B. A. Pailthorpe, and R. C. McPhedran, Aust. J. Phys. **44**, 73 (1991).

[15] R. Holm, *Electrical Contacts Handbook,* 3rd ed. (Springer-Verlag, Berlin, 1955); W. D. Collins, Proc. Edinburgh Math. Soc. **13**, 235 (1962).

[16] H. B. Dwight, J. Math. Phys. Cambridge, Mass. **10**, 50 (1931); D. Reitan and T. J. Higgins, Trans. Am. Inst. Electr. Eng. **75**, 761 (1957); F. H. Murray, J. Math. Phys. Cambridge, Mass. **12**, 306 (1933); E. Hallen, Ark. Math. Ast. Phys. **21**, 1 (1929); G. Howe, Electrician No. 9, 906 (1914).

[17] J. Rauch and M. Taylor, J. Math. Phys. **16**, 284 (1975).

[18] M. Von Smoluchowski, Z. Phys. Chem. **92**, 129 (1917); F. C. Collins and G. E. Kimball, J. Colloid Sci. **4**, 425 (1949); see Ref. [25].

[19] (a) F. Spitzer, Z. Wahr. **3**, 110 (1964); (b) R. K. Getoor, *ibid.* **4**, 248 (1965); (c) W. Thomson, Philos. Mag. **7**, 192 (1854).

[20] H. S. Carslaw, Proc. R. Soc. Edinburgh **61**, 223 (1943).

[21] J. D. Jackson, *Classical Electrodynamics* (Wiley, New York, 1962).

[22] J. Happel and H. Brenner, *Low Reynolds Number Hydrodynamics* (Noordhoff, Leyden, 1973).

[23] M. Gordon, S. C. Hunter, J. A. Love, and T. C. Ward, Nature **217**, 735 (1968). The force per unit displacement of an inclusion embedded in an incompressible sticking elastic medium obeys an expression of the form (1.3), where the solvent viscosity η_s is replaced by shear modulus G.

[24] L. E. Payne and W. H. Pell, J. Fluid Mech. **1**, 529 (1960). Payne and Pell derive an analog of (1.4b) for the friction of axisymmetric bodies moving along their axis of symmetry.

[25] (a) H. C. Berg and E. M. Purcell, Biophys. J. **20**, 193 (1977); (b) D. Shoup and A. Szabo, *ibid.* **43**, 33 (1982); (c) B. Goldstein and F. W. Wiegel, *ibid.* **43**, 121 (1983).

[26] J. B. Hubbard and J. F. Doulgas, Phys. Rev. E **47**, 2983 (1993).

[27] B. A. Luty, J. A. McCammon, and H.-X. Zhou, J. Chem. Phys. **97**, 5682 (1992).

[28] D. L. Ermak and J. A. McCammon, J. Chem. Phys. **69**, 1352 (1978).

[29] H.-X. Zhou, A. Szabo, J. F. Douglas, and J. B. Hubbard, J. Chem. Phys. **100**, 3821 (1994).

[30] The original Brownian dynamics algorithm of Luty, McCammon, and Zhou (Ref. [27]) involved an additional spherical surface outside $r = b$. When the Brownian particle reached this larger surface, it was tested whether the particle should be labeled as escaping to infinity or put back to the b surface. Here this procedure is modified so that every time the particle crosses the b surface the test is done right away. This modification makes the algorithm conceptually simpler and more efficient.

[31] M. Takiya, J. Chem. Phys. **69**, 2375 (1978). This work discusses the probabilistic interpretation of capacity from a physical chemistry perspective.

[32] J. G. Kirkwood and J. Riseman, J. Chem. Phys. **16**, 565 (1948); J. W. Miles, J. Appl. Phys. **38**, 192 (1967). Miles develops an electrostatic slender body theory analogous to the KR theory.

[33] H. Yamakawa, *Modern Theory of Polymer Solutions* (Harper and Row, New York, 1971).

[34] D. K. Reitan and T. J. Higgins, J. Appl. Phys. **22**, 223 (1951). This work mentions a comment by Kirchhoff that Dirichlet solved the exterior Dirichlet problem for a cube shortly before Dirichlet's death. Dirichlet's research on this question has apparently been lost. (See also Ref. 1).

[35] G. D. Cochran, Ph.D. thesis, University of Michigan, 1967.

[36] M. L. Glasser and J. J. Zucker, Proc. Natl. Acad. Sci. (U.S.A.) **74**, 1800 (1977). P. G. Doyle and J. L. Snell, *Random Walks and Electrical Networks,* Carus Monograph No. 22 (Mathematical Association of America, Washington, D.C., 1984). The conjecture (3.1c) derives from the correspondence between the number of distinct sites visited by a random walk S_n and the volume of the Wiener sausage [19]. Glasser and Zucker show that S_n on a cubic lattice scales as $S_n \sim C_L n$, where C_L is the conjectured capacitance of a unit cube in Eq. (3.1c). C_L has numerous physical applications: (i) critical binding energy of electrons to defect sites [G. F. Koster and J. C. Slater, Phys. Rev. **96**, 1208 (1954)] and impurity atom localization [T. Kotera, Prog. Theor. Phys. Suppl. **23**, 141 (1962)]; (ii) critical temperature of the spherical model [G. S. Joyce, J. Phys. A **5**, L65 (1972)]; (iii) mean dimensions of networks of flexible polymer chains [B. E. Eichinger, J. Chem. Phys. **65**, 2041 (1976)]; and (iv) resistance of networks of resistors [G. Vineyard, J. Math. Phys. **4**, 1191 (1963)].

[37] C. Snow, J. Res. Natl. Bur. Stand. **43**, 377 (1949); H. M. MacDonald, Proc. Lond. Math. Soc. **26**, 156 (1895); M. Schiffman and D. C. Spencer, Q. J. Appl. Math. **5**, 270 (1947); S. Wakiya, Arch. Mech. (Warsaw) **32**, 809 (1980).

[38] G. Dassios and R. E. Kleinman, Q. J. Math. **212**, 467 (1989); A. R. Rosen, J. Inst. Math. Appl. **9**, 2801 (1972); V. Erma, J. Math. Phys. **4**, 1517 (1963). Erma develops a perturbation theory of capacity using a spherical harmonic expansion of the surface.

[39] O. A. Ladyzhenskaya, *The Mathematical Theory of Viscous Incompressible Flow* (Gordon and Breach, New York, 1963); Ladyzhenskaya shows that the velocity field for a Stokes flow can be represented by a distribution of beads on the surface of the body; see also N. S. Clarke, J. Fluid Mech. **52**, 781 (1972).

[40] E. Swanson, D. C. Teller, and C. deHaën, J. Chem. Phys. **72**, 1623 (1980).

[41] J. Rotne and S. Prager, J. Chem. Phys. **50**, 4831 (1969).

[42] J. Garcia de la Torre and V. M. Bloomfield, Q. Rev. Biophys. **14**, 81 (1991).

[43] V. Bloomfield, W. O. Dalton, and K. E. Van Holde, Biopolymers **5**, 135 (1987).

[44] S.-Q. Wang, J. F. Douglas, and K. F. Freed, J. Chem. Phys. **85**, 3674 (1986); **87**, 1346 (1987).

[45] R. W. Pastor and R. Zwanzig, J. Chem. Phys. **90**, 5729 (1989).

[46] R. Zwanzig, Proc. Natl. Acad. Sci. (U.S.A.) **87**, 5856 (1990).

[47] S. H. Northrup, J. Phys. Chem. **92**, 5847 (1988).

[48] J. M. Burgers, in *Second Report on Viscosity and Plasticity* (Amsterdam Academy of Science, Amsterdam, 1938).

[49] H. A. Kramers, Physica **1**, 245 (1940); J. Chem. Phys. **14**, 415 (1946).

[50] P. Debye, J. Chem. Phys. **14**, 636 (1946).

[51] P. E. Rouse, J. Chem. Phys. **21**, 1272 (1953).

[52] E. Swanson, D. C. Teller, and C. de Haën, J. Chem. Phys.

68, 5097 (1978).

[53] B. H. Zimm, Macromolecules **13**, 592 (1980).

[54] J. G. de la Torre, A. Jimenez, and J. Freire, Macromolecules **15**, 148 (1982); J. M. Garcia Bernal, M. M. Tirada, J. J. Freire, and J. G. de la Torre, *ibid.* **24**, 593 (1991); C. Camacho and M. E. Fisher, Phys. Rev. Lett. **65**, 9 (1990).

[55] S. Park, T. Chang, and I. H. Park, Macromolecules **24**, 5729 (1991); M. Schmidt and W. Burchard, *ibid.* **14**, 210 (1981).

[56] M. Fixman, J. Chem. Phys. **80**, 6324 (1984).

[57] C. M. Guttman, F. L. McCrackin, and C. Han, Macromolecules **15**, 1205 (1982); B. J. Cherayil, J. F. Douglas, and K. F. Freed, J. Chem. Phys. **83**, 5293 (1985); **87**, 3089 (1987); S. J. Chen and G. C. Berry, Polymer **31**, 733 (1990).

[58] J. F. Douglas, J. Roovers, and K. F. Freed, Macromolecules **23**, 4168 (1990); K. F. Freed, S.-Q. Wang, J. Roovers, and J. F. Douglas, *ibid.* **21**, 2219 (1988).

[59] J. F. Douglas and K. F. Freed, Macromolecules **17**, 2344 (1984); **18**, 201 (1985).

[60] S.-Q. Wang, J. F. Douglas, and K. F. Freed, Macromolecules **18**, 2464 (1985).

[61] J. M. G. Bernal, M. M. Tirado, J. J. Freire, and J. G. de la Torre, *ibid.* **24**, 593 (1991).

[62] P. Debye and A. M. Bueche, J. Chem. Phys. **16**, 573 (1948).

[63] A. M. Berezhkovskii, Y. A. Makhnovskii, and R. A. Suris, J. Stat. Phys. **57**, 333 (1989); N. J. Jain and W. E. Pruitt, J. Anal. Math. **24**, 369 (1971).

[64] M. D. Donsker and S. R. S. Varadhan, Commun. Pure Appl. Math. **28**, 1 (1975); **28**, 279 (1975); **28**, 525 (1975); **32**, 721 (1979). The constant λ_d equals $[(d+2)/2](\lambda_0/d)^{d/(d+2)}$, where λ_0 is the lowest eigenvalue of ∇^2 [M. Robnik, J. Phys. A **13**, L349 (1980)].

[65] H. B. Rosenstock, Phys. Rev. **187**, 1166 (1969).

[66] R. E. Goldstein, T. C. Halsey, and M. Leibig, Phys. Rev. Lett. **66**, 1551 (1991); B. Duplantier, Phys. Rev. Lett. **66**, 1555 (1991). Calculation of the electrostatic free energy of an arbitrarily shaped charged colloid particle in an electrolyte solution also involves the exterior Dirichlet problem for the diffusion equation. The linearized Poisson-Boltzmann equation corresponds to the Laplace transform of the diffusion equation where the conjugate variable to time t is the inverse square Debye screening length. We also mention that the Born estimate of the solvation energy of ions is inversely proportional to the capacity of the cavity formed by the ion in the solvent [see A. A. Rashin and B. Honig, J. Phys. Chem. **89**, 5588 (1985)]. Born model calculations conventionally assume a spherical cavity.

[67] S. Port, in *Random Walks, Brownian Motion and Interacting Particle Systems,* edited by R. Durrett and H. Kesten (Birkhäuser, Boston, 1991), p. 375–388.

[68] J. Le Gall, Ann. Prob. **16**, 991 (1988); J. F. Douglas, Macromolecules **22**, 1786 (1989). The geometrical interpretation of the "fractal dimension" ϕ is discussed by J. Rosen, Commun. Math. Phys. **88**, 327 (1983).

[69] A. Dvoretsky, P. Erdös, and S. Kakutani, Acta Sci. Math. B (Szeged.) **12**, 75 (1950); O. D. Kellogg, *Foundations of Potential Theory* (Springer-Verlag, Berlin, 1929), p. 331. The capacity of any finite collection of smooth arcs vanishes in $d=3$.

[70] (a) H.-X. Zhou and A. Szabo (unpublished); (b) D. Shoup and A. Szabo, J. Electroanal. Chem. **140**, 2371 (1982).

[71] J. Boussinesq, *Théorie Analytique de la Chaleur, II* (Gauthiers-Villars, Paris, 1903), p. 224; Compt. Rend. **100**, 935 (1885); L. D. Landau and E. M. Lifshitz, *Fluid Mechanics* (Addison-Wesley, Reading, MA, 1959), p. 96; C. J. Lawrence and S. Weinbaum, J. Fluid Mech. **171**, 209 (1986); A. B. Basset, Philos. Trans. R. Soc. London **179**, 43 (1888).

[72] H. Levine, J. Fluid Mech. **3**, 145 (1958). See the bottom of p. 146 for a discussion of the analogy between skin friction and heat flux.

[73] G. K. Batchelor, Q. J. Appl. Math. **7**, 179 (1954).

[74] J. W. S. Rayleigh, Philos. Mag. **21**, 697 (1911).

[75] A. J. Barrett and B. C. Benesch, J. Chem. Phys. **97**, 9454 (1992).

[76] G. Weiss and L. E. Payne, J. Appl. Phys. **25**, 1351 (1954). Such dimensional shifts ($d \rightarrow d+2$) relating hydrodynamic and electrostatic problems occur frequently in generalized axisymmetric potential theory [77].

[77] L. E. Payne, Q. Appl. Math. **10**, 197 (1952); A. Weinstein, Bull. Am. Math. Soc. **50**, 20 (1953); L. E. Payne and A. Weinstein, Pacific J. Math. **2**, 633 (1952); R. P. Kanwal, J. Fluid Mech. **10**, 17 (1960); R. P. Roscoe, Philos. Mag. **40**, 338 (1949). The rotational friction of an arbitrarily shaped lamina about an axis normal to the plane defining the lamina can also be calculated using an electrostatic analog.

[78] G. I. Taylor, Proc. R. Soc. London Ser. A **70**, 13 (1928); G. Birkhoff, *Hydrodynamics* (Princeton University Press, Princeton, 1950).

[79] B. J. Berne, J. Chem. Phys. **56**, 2164 (1972); S. C. Szu and J. J. Hermans, J. Fluid Mech. **66**, 385 (1974).